

Daniel Zaszewski¹, Tomasz Gruszczyński²

A Low-cost Automatic System for Long-term Observations of Soil Temperature


Abstract: The description of the physical parameters characterizing heat transport in the soil medium, especially on a regional scale, requires long-term and high frequency observations of temperature changes in soil profiles. This paper presents a project for a multi-channel, modular and universal data logger for temperature distribution data collecting in the soil profile, based on open electronic components, such as Arduino microcontroller systems and DS18B20 thermometers. The data logger tests were carried out in two profiles. The seven-month tests did not show any errors in the functioning of the measurement set. The presented device requires an average current of 320 μA , which allows for its stable operation on one battery set for about 300 days in temperate climate conditions. The DS18B20 thermometers allow for accurate and stable temperature measurement (the mean absolute error after laboratory calibration was 0.02°C). The cost of a single measurement-registration device was approximately 76 EUR, representing a competitive price in comparison with commercial data loggers. This allows, with relatively low expenditure, the creation of extensive observation networks for the analysis of the heat flow process in high temporal and spatial resolution.

Keywords: data logger, Arduino boards, soil temperature, heat transport, DS18B20 digital thermometers

Received: 30 March 2022; accepted: 17 October 2022

© 2023 Author(s). This is an open access publication, which can be used, distributed and reproduced in any medium according to the Creative Commons CC-BY 4.0 License.

¹ University of Warsaw, Faculty of Geology, Warsaw, Poland, email: danielzaszewski@uw.edu.pl,
 <https://orcid.org/0000-0003-0830-8547>

² University of Warsaw, Faculty of Geology, Warsaw, Poland, email: tgruszcz@uw.edu.pl,
 <https://orcid.org/0000-0002-3621-3644>

1. Introduction

The thermal monitoring of a soil medium is of particular importance in the context of geothermal resources since the datasets of soil temperature are used, among others, to identify zones convenient for the location of heat exchangers [1]. As well as in model tests allowing for the estimation of thermal parameters of the bedrock [2–4]. In deep geothermal systems, the steady state condition of the system is taken into account. In turn, in shallow geothermal systems, the process of heat transport occurs in reference to the zone of seasonal fluctuations and should be subject to a transient approach [5]. This stems from the fact that heat flow in this zone may be analyzed as a phenomenon of heat wave propagation, generated due to the repeatable warming and cooling of the Earth's surface. Additionally, the temperature signal is considered to be a superposition of signals characterized by different frequencies (e.g. temperature oscillations in daily and annual cycles). Therefore, a mathematical model with a high temporal resolution, one in which the role of the state function is played by soil temperature, is commonly applied to describe heat transfer [6]. This means that the calibration procedure of such a model requires long-term and high-frequency temperature measurements, and thus involves the organization of a network of multichannel environmental dataloggers.

Commercial solutions for data logging, although characterized by high quality and reliability, are expensive. For multi-channel data loggers, the cost of the cheapest models available on the market (without a set of sensors) starts at around 250 EUR [7, 8]. Alternatives to multi-channel dataloggers include cheaper and sensor-integrated single-channel designs, e.g. iButton [9, 10]. The construction of large measurement networks necessitates the purchase of multiple devices which may exceed the cost of a multi-channel data logger and also multiplies the inconvenience of handling them. The design of such data loggers can limit or sometimes prevent their use in some research works. For example, the aforementioned iButton requires disassembly each time in order to read the data. This limits its suitability for long-term observations of soil temperature.

Individual cost still remains the main barrier in the implementation of a data logging system, particularly in pilot projects. This leads to the restriction of the number of units used and a decrease in the spectrum of the accumulated datasets [11].

There is increasing interest in the construction of electronic circuits in the framework of the citizen-science movement, leading to those based on easily configured, open prototype systems such as Arduino, and giving the opportunity to design and create a logging system with parameters close to its commercial equivalents. The project may be supported by a broad community of companies, organizations, and users, mutually sharing their observations and solutions. In this case, even an early-stage researcher without a background in electronic engineering may have access to numerous electronic components, computer software libraries, and demonstrative software to implement their given project. Examples of systems logging and

preserving environmental data, constructed on the basis of open electronic components, have been presented by Gandra et al. [11], Ferlan and Simončič [12], Lockridge et al. [13], Akhter et al. [14], Fisher et al. [15] and Medojevic et al. [16]. The study of Beddows and Mallon [17] and E. Mallon's blog [18], were extremely useful during the construction and programming stages of the data logger presented in this work.

2. Materials and Methods

The construction of the system, comprising temperature sensors and a data logger, was based on the following assumptions:

- stable work of the data logger at variable thermal and humidity conditions,
- low power consumption / long working period with the application of a single power source,
- high accuracy of temperature measurements coupled with insignificant drift,
- possibility of temperature measurement from at least seven sensors, located according to the requisite WMO standards [19],
- maintaining stable sampling time,
- low production cost of the data logger.

2.1. Microcontroller Board – Arduino Pro Mini

The central part of the data logger is a module containing a microcontroller which supervises the work of the device and receives signals from the periphery circuits. The Arduino Pro Mini module by Sparkfun was used in this project. These microcontrollers are low-cost and easy to program. The Arduino hardware and software platform [20] has an extensive community that provides support for learning and troubleshooting. The Arduino Pro Mini contains an 8-bit Atmel ATmega328P microprocessor with a clock frequency of 8 MHz and operates at 3.3 V logic levels (power supply of integrated circuits and their logic levels are referred to 3.3 V). The microcontroller has an integrated 32 kB Flash memory, 1 kB EEPROM memory and 2 kB SRAM memory [21].

Arduino Pro Mini only contains the basic electronic components allowing for microcontroller operation, such voltage regulator, crystal oscillator, necessary resistors and capacitors. The USB/UART converter was not installed, which on one hand reduces power consumption related with circuit operation and on the other hand reduces the dimensions of the device [17]. For minimization of power consumption by the module, resistors with two signal LEDs were removed from the original circuit board (Fig. 1a).

2.2. Real Time Clock (RTC)

Maintenance of high precision of data logging time measurements is a crucial aspect during long-term observations. Precise RTC circuits enable the reduction of the need for any intervention in the code for synchronization with reference clocks.

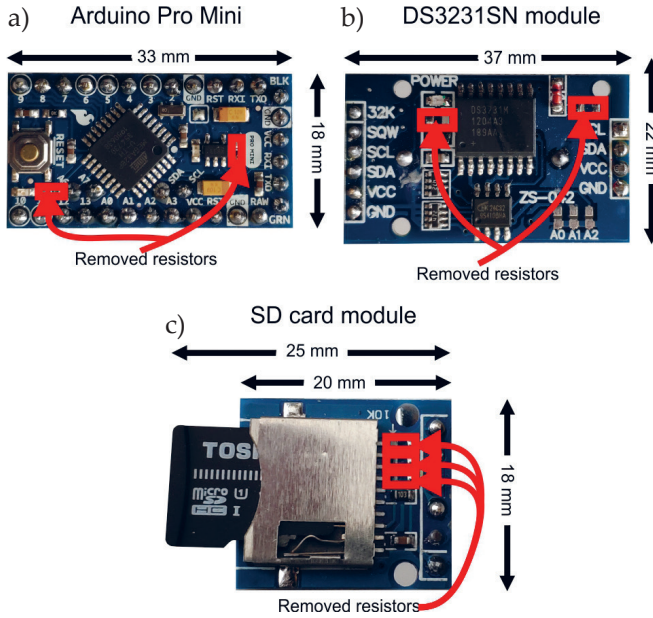


Fig. 1. Arduino Pro Mini board prepared for use in the data logger (a); DS3231 real time clock module with AT24C42 EEPROM memory chip (b); Micro SD card module (c) with marked resistors to be removed

The RTC applied in the project is a DS3231 by Maxim Integrated. This is a popular and cheap circuit, composed of an integrated 32 kHz crystal oscillator with temperature compensation. Temperature measurements by the built-in sensor and automatic corrections allow the maintenance of a resolution at ± 2 ppm (at 0–40°C) and 3.5 ppm (in the range from -40 to 0°C and from 40 to 85°C) [22, 23]. With regard to the synchronization time, this amounts to about 2 minutes annually.

The DS3231 communicates with the microcontroller using an Inter-Integrated Circuit (I²C) serial interface. The DS3231 chip has the function of generating a signal at a strictly user-defined [23]. This signal, when applied to the appropriate microcontroller pin, can wake the microcontroller from a low-power state. It is therefore a key component of the data logger, allowing it to operate significantly longer on battery power sources. During any event of a lack of power supply from the main source, DS3231 registers may be sustained using a CR2032 battery.

The project uses a system equipped with RTC DS3231, EEPROM memory chip – AT24C32 and a set of components and input/output (IO) connections, enabling a direct connection with the microcontroller board (Fig. 1b). The resistor sustaining LED operations (informing of the clock operation) and the resistor connected to the LIR2032 accumulator charging circuit (used for emergency power supply), which is ineffective at 3.3 V [17], have both been removed from the circuits for the optimization of power consumption by the RTC module.

2.3. SD Card Module

Data acquired by the circuit is recorded on an SD card. The power supply of the data logging on the card is maintained at 3.3 V, which eliminates the need of using voltage converters in the device [24]. Communication between the microcontroller and the card is maintained by a serial peripheral interface (SPI), which is dedicated for peripherals requiring large data transfer speeds.

The Micro SD slots used in the project have SPI interfaces, 10 k Ω pull-up resistors and a voltage stabilizing capacitor (Fig. 1c). The pull-up resistors for SPI interfaces: MISO (Master Input Slave Output), MOSI (Master Output Slave Input) and SCK (clock), could be removed because the Arduino Pro Mini module contains internal resistors pulling up voltage to the pins. Moreover, retaining the resistor connected with the SCK could have caused stable power consumption even in the microcontroller sleep mode [17]. The data logger presented here uses Toshiba SDHC cards with a capacity of 16 GB. Although this capacity exceeds the assumed memory requirements for acquisition and record storage, it is currently the standard and therefore cheapest memory capacity in the new SD cards.

2.4. Soil Temperature Sensor

The temperature sensors DS18B20 designed by Dallas Semiconductor were used in the device. Due to their low cost, good degree of precision and operation stability, these sensors have gained a large following of adherents. These are digital sensors that generate temperature values without having to calculate them from an analogue signal (as is the case with sensors such as the LM35, TMP36 or thermistors) and using a noise-sensitive analogue-to-digital converter. Compared to other digital sensors (such as the MCP35, MCP9808, ADT7410, TMP117AIDRVR), they have a communication interface that allows data transmission over long distances from the recorder. DS18B20 sensors are used in engineering projects (e.g. for temperature monitoring in hydrotechnical devices [25], studies of concrete properties [26], industrial pipelines [27], geothermal installations [28, 29], environmental temperature (e.g. measurements of substrate temperature [5, 12, 14–16, 30–32]) and in karst hydrogeology [17].

The DS18B20 thermometer measures temperatures in the range of -55 to 125°C [33]. The sensor allows the measuring of temperatures with a resolution of 9 to 12 bits (0.5 – 0.0625°C). Communication between the microcontroller and the sensor takes place through a 1-Wire interface. This is a hierarchical serial interface allowing the control of numerous sensors (in the slave rank) by one master device. The communication is maintained by one data line (DQ), to which voltage should be pulled up through a 4.7 k Ω resistor, and the ground line (GND), which is the voltage reference level. The maximal distance between the logger and the sensor may reach about 300 m in perfect conditions. Nevertheless, in the case of such long measurement lines, the values of pull-up resistors should be decreased in order to supply power with a required current of 1.5 mA to the devices [33].

The sensor module contains three leads (Fig. 2): a power line (VCC), a ground line and a data line. For operations, the DS18B20 requires a stable voltage in the range of 3.0 to 5.5 V [33]. The factory calibration of the DS18B20 assures a temperature measurement at 0.5°C (in the range from -10 to 85°C). The guaranteed accuracy is, however, too low with regard to the requirements of standard observation networks determined by WMO and reaching the level of at least 0.2°C [19]. The high degree of stability of the temperature sensor circuit, however, allows for the increase of measurement accuracy in the process of external calibration [34].

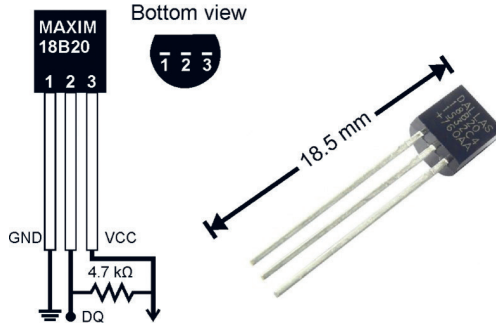


Fig. 2. DS18B20 temperature sensor in TO-92 housing, module view and connection diagram (VCC – power line, GND – ground line, DQ – data line).
The 4.7 kΩ resistor is a pull-up resistor, forcing the DQ line to high state.
The use of this resistor is required for the 1-Wire interface

2.5. Data Logger Unit Assembly

To maintain a stable and durable platform for the assembly of the electronic components of the logger circuit, a two-layer printed circuit board (PCB) was designed. The electronical scheme and PCB design files are available in the Mendeley data repository [35]. The PCB dimensions are 85 mm × 55 mm (Fig. 3a1, a2). Such dimensions allow for the comfortable distribution of the circuit components and mounting electric pathways, while at the same time guaranteeing the small dimensions of the device. Pin header slots with 2.54 mm spacing were used to mount the Arduino Pro Mini, RTC DS3231 modules and the SD card; they allow for the comfortable replacement of the modules in case of damage.

The following components were permanently mounted on the PCB (Fig. 3b1, b2):

- power supply slot DC 5.5 mm × 2.1 mm,
- connectors with 2.54 mm spacing for 7 DS18B20 sensors with 4.7 kΩ pull-up resistors,
- switches for particular 1-Wire outputs,
- connectors for programming, SPI and I2C interfaces,
- RGB signal LED with 30 kΩ resistor,
- resistors and capacitor for voltage divider.

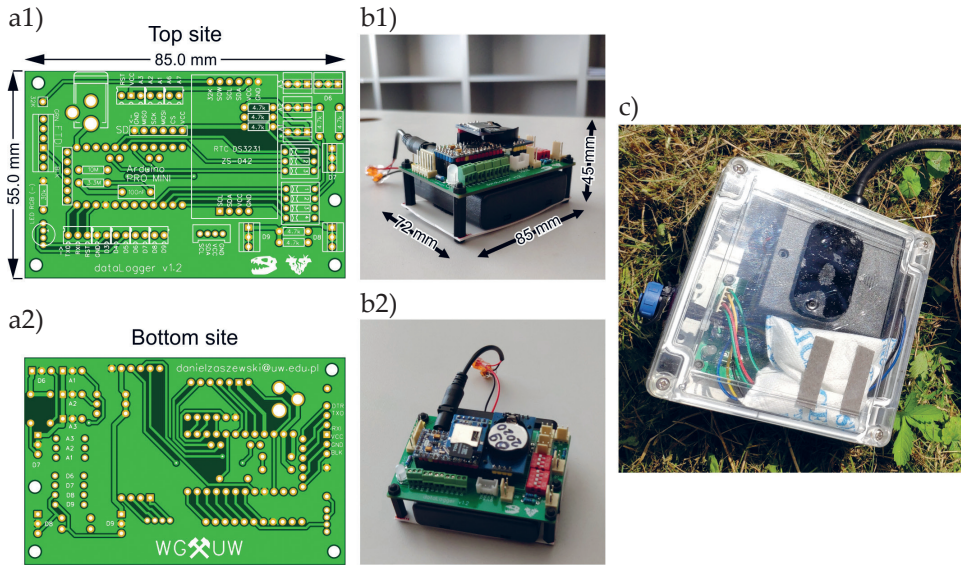


Fig. 3. Views of the PCB top and bottom side (a1 and a2); example of the data logger unit with mounted modules and electronic components (b1 and b2); data logger in PVC case (c)

Most of the Arduino pins (with the exception of the pins dedicated to I2C, SPI and UART communication) had an ARK screw terminal output, which allows the device to be used at a different pin configuration and/or with another set of periphery modules than in the originally designed circuit.

The entire device was inserted in a 120 mm × 120 mm × 60 mm hermetic PVC case (Fig. 3c) with a transparent cover (to ensure LED observation). Two openings were made in the case for the hermetic programmer joint output and the cable grommet for the cable with thermometers. To reduce the risk of water vapor condensation in the device, humidity absorbents in form of small silica gel bags were inserted into it. In addition, communication with the device and data download is via an airtight connector. This allows for connection to a PC via an interface equipped with a USB/UART converter, for example a CH340G. As a result, there is no need to open the housing, which protects the logger against moisture and dirt.

The set of thermometers used for the survey were mounted on one three-wire electric cable in a chain system. This configuration necessitated the use of a single pin for communication with the data logger. Each DS18B20 sensor was installed in a 6 mm × 30 mm cylindrical stainless-steel housing (Fig. 4b1–b3). To remove air from the space between the sensor and the enclosure walls, it was filled with thermally conductive paste. The connectors between the main cable and the thermometer outputs were placed in a housing made of a PVC cable gland with a sealing clamp. Such an enclosure protects the connector and thermometer from mechanical damage. It also serves as a form for the epoxy filler, which seals and stabilizes the connection

after hardening. The main electric cable was selected for the coating's resistance to external influences, particularly to soil moisture. The cable used was an OZ-600 control and installation cable with an external diameter of 6.5 mm and a PVC insulation that retains flexibility in the temperature range between -15 and 80°C and is resistant to organic and inorganic compounds. The cable has three numbered wires with a cross-section of 0.5 mm^2 .

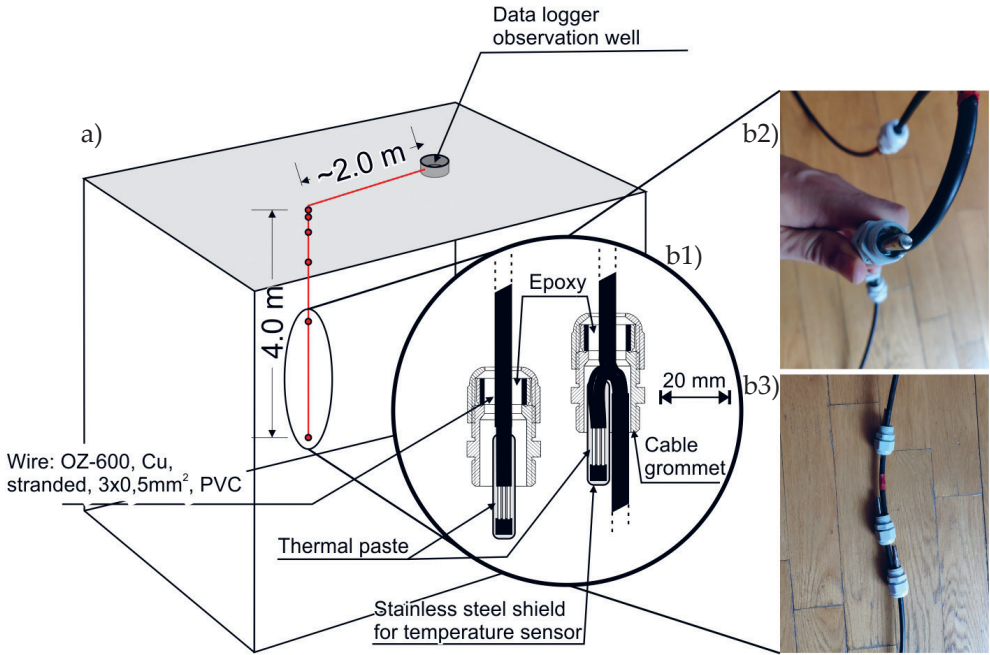


Fig. 4. The concept of the measurement system foundation in the test profile (a) and diagram of DS18B20 sensors line assembly (b1–b3)

The sensor placement interval on the main cable was adapted to the WMO standards, and extended to include sensors recording temperature at 2.0 and 4.0 m depth levels (Fig. 4a). In addition to the case, the data logger was installed in a covered observation well made of PVC, each being 20 cm high and 20 cm in diameter. To reduce the influence of the observation well on the readings of the shallow thermometers, it was mounted at a distance of no less than 2.0 m from the sensor line.

The devices constructed in the presented project are supplied by a source with 6 V voltage. This was achieved by using four series-connected Energizer Ultimate Lithium 1.5 V AA batteries. As the applied microcontroller requires a voltage of 3.3 V, the system uses the MIC5205 voltage regulator built into the Arduino Pro Mini board. Due to the high probability of sub-zero temperatures in the winter season, lithium batteries were utilized; they can operate without large capacity loss in the range from -35 to 65°C temperature range [36].

2.6. Software

The advantage of working with open modules or those conforming to the Arduino standard is the possibility of programming microcontrollers using a dedicated, multi-platform, simple in operation Arduino IDE integrated software environment [20]. This program contains the functions of code editor, compiler and uploader used to upload the program on a selected microcontroller. Arduino IDE allows the creation of programs (sketches) in a language which is a derivative of C++.

The program code implemented in this project is based on the sketch developed by E. Mallon for The Cave Perl Project [18]. The code was modified for adjustment to the specifics of soil temperature measurements. The program code can be found in the Mendeley Data repository at <https://data.mendeley.com/datasets/k5w4v6h5cp> [35].

The code has changed the system for saving and reading data on the SD card. The data is stored in a single *.csv file, allowing the contents of the file to be read directly without removing the card. Support for multiple DS18B20 sensors installed on one or 7 data buses was implemented in the code. The resources of the Dallas Temperature library [37] were used to support the sensors and the 1-Wire interface.

2.7. Calibration of the Temperature Sensors

The DS18B20 sensor sets were subject to calibration with the application of a precision thermometer connected with a Termio-1 data logger by TERMOPRODUKT, equipped with a platinum temperature sensor PT1000. The reference thermometer had an accuracy of 0.05°C in the temperature range of 0–50°C. The instrument precision was 0.01°C. Calibrations were performed in laboratory conditions in a water bath. The range of water temperatures during the measurements was from 2.9 to 22.1°C, and corresponded to the thermal expectations in the analyzed soil profiles. The measurements were made every 5 min, which resulted in 61 temperature readings for each sensor and for the reference thermometer. Thus, observation vectors were obtained which could be used to analyze the distribution of the residual component, i.e. the difference between the temperature from the sensor and the corresponding temperature from Termio-1.

2.8. Field Testing

Data logger and sensors tests were performed in two study sites located in central Poland (Fig. 5a). The use of two instruments allowed observations to be made in different geological settings. When selecting a test point, care was taken to ensure that the sediments were homogeneous as possible. At the same time, the sediments should differ significantly in thermal diffusivity values and represent lithological types frequently found in the Polish Lowlands. The first test device was installed in a rural area in Bobrowce (Fig. 5b–d), in a 4.0-metre deep profile, in which fine-grained sands with small admixture of gravels and medium- to coarse-grained sands were drilled. A similar test device was installed in an urban area (Warsaw city, Fig. 5e, f), in a profile composed of clay sands and sandy clays. The sampling intervals were assumed at one measurement per 10 min.

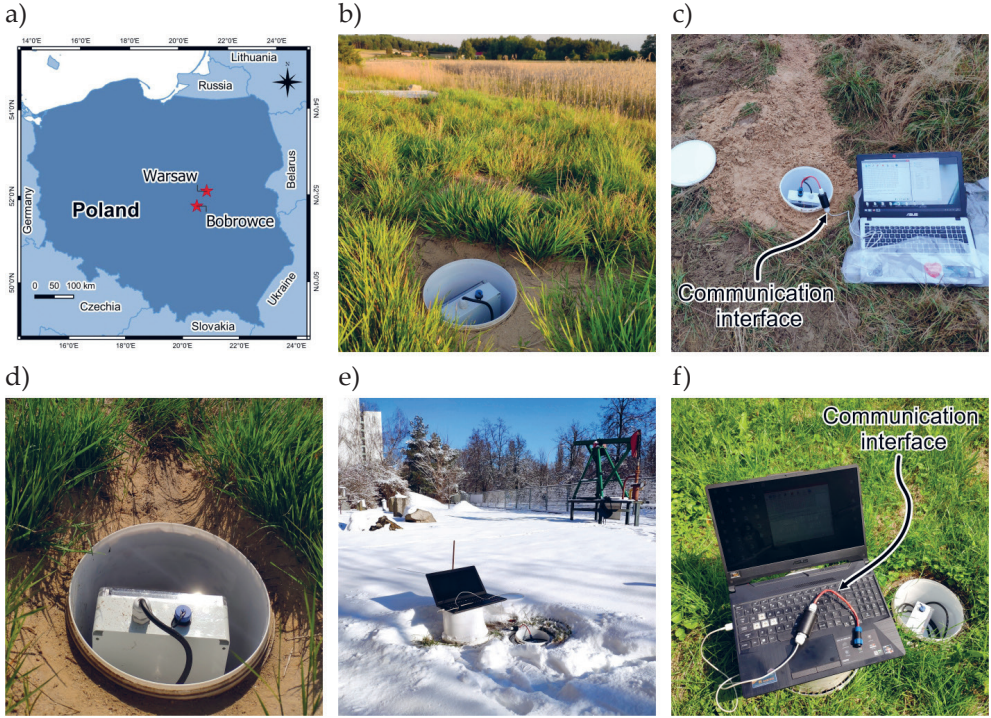


Fig. 5. Location (a) and photographs of the Bobrowce (b–d) and Warsaw (e, f) study sites

The tests were conducted between the autumn of 2020 and the summer of 2021. The presented results of the data logger tests include the interval between the installation of the devices, i.e. from 7.11.2020 (Bobrowce) and 1.12.2020 (Warsaw) to 1.07.2021.

The functioning of the DS18B20 sensor circuit was assessed in field conditions based on a mathematical model of heat transfer in a soil profile. To achieve this, a finite difference method was used, which is a numerical, estimated solution of a univariate equation of heat diffusion in a transient state:

$$\lambda \frac{\partial^2 T}{\partial z^2} = c_p \rho \frac{\partial T}{\partial t} \tag{1}$$

where:

- T – medium temperature [°C],
- λ – thermal conductivity coefficient [W/(m·K)],
- c_p – specific heat [W/(kg·K)],
- ρ – density [kg/m³],
- z, t – variables of space and time, respectively.

Based on an implicit scheme, the differential analogue of this equation for a homogenous medium may be presented as:

$$\lambda \frac{T_{i-1,j+1} - 2T_{i,j+1} + T_{i+1,j+1}}{\Delta z^2} = c_p \rho \frac{T_{i,j+1} - T_{i,j}}{\Delta t} \quad (2)$$

where:

- i, j – indexes referring to points in space and time, respectively,
- Δz – space discretization step,
- Δt – time step.

It is possible to express a set of linear equations for each time step, which may be presented in matrix form:

$$\mathbf{A} \cdot \mathbf{h} = \mathbf{rhs} \quad (3)$$

where:

- \mathbf{A} – coefficient matrix,
- \mathbf{h} – vector of unknowns,
- \mathbf{rhs} – right hand side vector.

After formulating the boundary and initial conditions, the system may be solved sequentially with application of any iterative algorithm. It should be noted that the coefficient matrix is sparse and its non-zero elements are only grouped on three diagonals. Furthermore, at constant Δt , this matrix is unchangeable for each time step. This resulted in the possibility of developing an algorithm with high numerical efficiency, including the determination of a matrix inverse to \mathbf{A} . Such an approach allows us to resign from the iterative solution of equation (3) in each time step, and the vector of unknowns may be found directly from equation:

$$\mathbf{h} = \mathbf{rhs} \cdot \mathbf{A}^{-1} \quad (4)$$

This algorithm was implemented to the FloatBound software prepared in Python 3.7, with the application of NumPy library resources. The algorithm is characterized by its high degree of numerical effectiveness, and because it has to be performed only once during the calculations (matrix \mathbf{A}^{-1} is constant for each time step), it does not lose effectiveness even at high spatial and temporal resolutions of the calculations.

A heat conduction model was made for both study sites. The calculations were performed for a soil profile from the surface to the depth of 4.0 m. The same discretization step of 0.1 m was applied in the entire profile. Calculations were made with constant time step of 1 h between 1.12.2020 and 1.07.2021, comprising 5094 h in total. On both boundaries of the model, time-variable boundary conditions of first type were assumed. To achieve this, vectors of temperature observations obtained from

the logger at depth levels 0.05 and 4.0 m were used. To determine the initial conditions, temperature measurements from 1.12.2020 (at 00:00) from all seven sensors were applied.

3. Results and Discussion

3.1. Battery Life Estimation

The tests began with measuring the current draw by the registry circuit with the set of seven thermometers DS18B20. The measurements were made using a VOLCRAFT VC276TRMS multimeter. The sampling interval was 2 min. Figure 6 presents a chart of current draw by the logger system coupled with the DS18B20 sensors. It includes the time of instruction execution in the SETUP procedure of program code and three cycles of reading and saving from temperature sensors. The SETUP procedure lasted for approximately 34 s. The mean current draw at that time was 4.30 mA. A short-term pulse (18.19 mA) related with operations on the SD card, including creation of a new data file, is also visible. It should be emphasized, however, that the operation time of the SETUP procedure will increase with a larger dataset (for a longer observation period). Nevertheless, the procedure will rarely be performed and should not significantly influence the durability of the batteries. In the case when the correct loop of readings and record of the data from the thermometers is made, the operation time is 6 s. The mean current draw during logging is 4.40 mA. After the registration, there is a short-term (0.183 s) peak related with data saving on the SD card. Between acquisition intervals, the system is in the stand-by mode. The current measured during these intervals is 290 μ A.

In the case of the sampling interval, reaching 1 measurement per 10 min, data reading and saving for a sensor set counts up to about 1% of the entire operation in the LOOP procedure of program code. The weighted mean of current draw in such cycle is 0.32 mA.

The following equation was used to estimate the expected battery life time:

$$t_b = \frac{0.85C}{(t_w I_w + t_s I_s) / 3600000} \cdot \frac{1}{24} \quad (5)$$

where:

- t_b – battery life time [days],
- 0.85C – nominal battery capacity reduced by 15% for consideration of self-degradation [mAh],
- t_w – sampling time per hour [ms],
- I_w – mean current draw during logging [mA],
- t_s – sleep time per hour [ms],
- I_s – mean current draw during sleep [mA].

In ideal conditions of power source exploitation (fresh lithium batteries with rated capacity of 3000 mAh) [36], the estimated operation time on one battery set is 320 days. Change of thermal conditions during the device operation as well as procedures of microcontroller reset for data acquisition may significantly shorten this period. To ensure a fault-free and continuous data acquisition, we suggest battery exchange no less than once every 6 months.

The voltage of the battery set measured before the data loggers started operating was 7100 mV. After 180 days the voltage at the Bobrowce point was 6812 mV and at the Warsaw point it was 6851 mV. According to the datasheet [36], a sudden drop in voltage, indicating a low battery, will occur when the battery setpoint voltage drops to about 5600 mV. Once a value of 5600 mV is observed, immediate replacement of the entire battery pack should be considered.

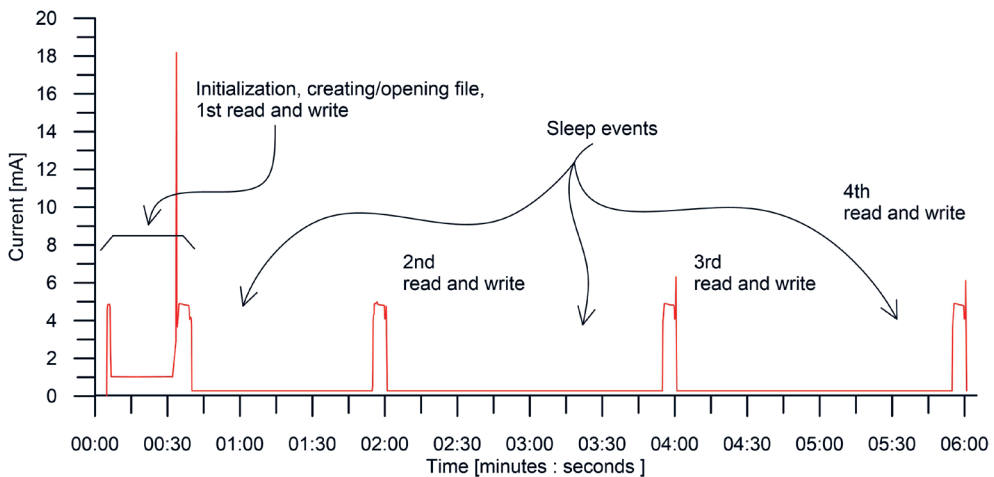


Fig. 6. Graph of current flow through the data logger and seven DS18B20 thermometers, with a 2-minute sampling interval

3.2. Accuracy of the Temperature Sensors

The process of sensor calibration was performed in laboratory conditions according to the method presented in Chapter 2.3. Values of differences between temperatures measured with application of DS18B20 sensors and the reference thermometer were in the range of -0.28 to 0.21°C (Fig. 7a, b). The mean measurement error for all sensors was -0.13°C , and the mean absolute error was 0.15°C . Errors observed in the analyzed temperature range (2.9 – 22.1°C) were lower from those declared by the producer, however they still exceeded the values recommended for standard environmental measurements [19].

In the calibration process, data measured by DS18B20 sensors were treated as predictor variables and temperatures measured with the reference thermometer

were outcome variables. The relationship between the indications of the DS18B20 sensors and the reference sensor showed a clear linear trend (Fig. 7c), therefore linear regression analysis was used for the quantitative description of relations between these variables. Examples of function parameters determined with the application of this method are presented in Table 1. The slopes for all sensors were positive and slightly exceeded 1 (1.01–1.02). This indicates the high degree of compatibility of the temperature change trend in both datasets; it should be expected that with temperature increase the sensors will have a tendency to show a decreased value with regard to the real value. This finds confirmation in the empirical distribution of the residual component (Fig. 7a, b). Intercepts of the equations mostly attained negative values (between -0.2 and 0.0°C). This means that the indications of most of the applied DS18B20 sensors will require correction by around 0.15°C . The R^2 coefficient for particular functions is close to 1, which indicates that the applied linear regression model well describes the relationship between temperature values obtained from sensors and the reference temperature.

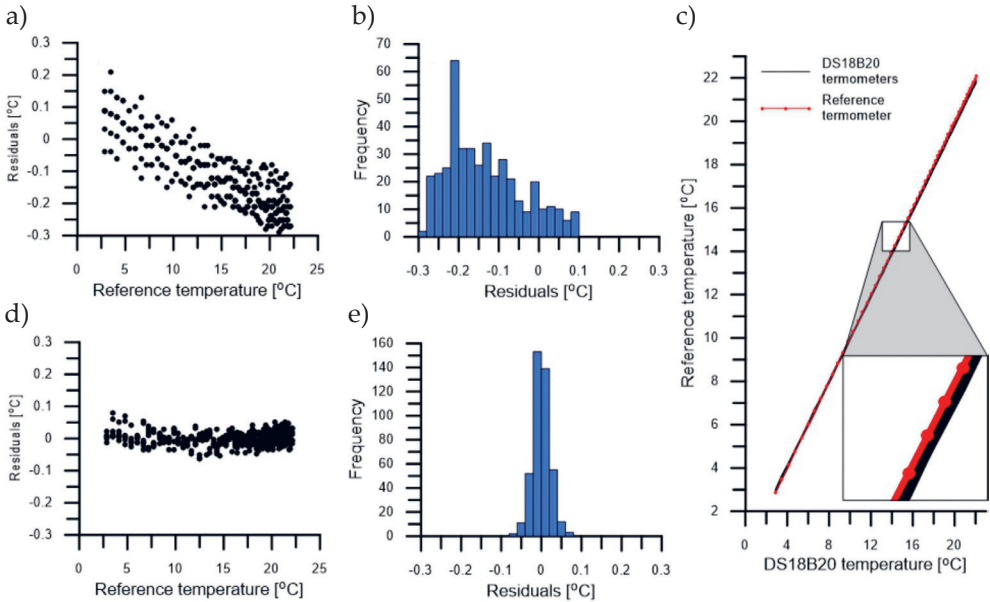


Fig. 7. Plot of residuals values to temperature measured by the reference thermometer (a) and histogram of residuals (b) before correction; correlation diagram between temperature values measured by DS18B20 sensors and the reference thermometer (c); relation of residuals values to temperature measured by the reference thermometer (d) and histogram of the residuals (e) after correction

After the application of corrective functions, a new dataset was obtained for which the residual values were calculated. They were in the range of -0.06 to 0.08°C , and the value distribution was close to a normal distribution (Fig. 7d, e). The mean

measurement error of all sensors was 0.0°C. After the calibration of 14 sensors, the obtained accuracy expressed as the mean absolute error value was 0.02°C, with the maximum residual at the level of 0.08°C. The measurement resolution ranged from 0.0632 to 0.0636°C and only slightly differed from the factory resolution of the DS18B20 sensor (0.0625°C). The accuracy of the DS18B20 sensors indications obtained through calibration is considered appropriate for the survey in the expected temperature range of the soil medium.

Table 1. Slopes and intercepts for regression curves obtained in the DS18B20 sensors calibration process for the Bobrowce profile

Sensor number	Slope	Intercept [°C]	R ²
1	1.0118	0.0071	0.9999
2	1.0186	-0.1408	0.9996
3	1.0172	-0.1352	0.9998
4	1.0160	-0.1908	0.9998
5	1.0189	-0.1584	0.9997
6	1.0169	-0.1284	0.9998
7	1.0153	-0.0515	0.9999

3.3. Field Tests

The variability of weather conditions during the tests allowed for observation how the data logger operates at low and high temperatures. The lowest values registered by the weather station of IMGW (Institute of Meteorology and Water Management) Warszawa-Okęcie occurred in: 8–21.01.2021, 28.01–2.02.2021 and 4–19.02.2021 (Fig. 8c), when the minimal temperatures reached down to -20.6°C (18.01.2021). Three cycles of snow cover formation and melting were also observed (13–23.01.2021, 26.01–03.02.2021 and 9–22.02.2021); its thickness reached 14 cm (Fig. 8c). The highest temperatures were observed in June, with values exceeding 25°C during the day.

No logger failure was observed during the tests (Fig. 8a, b). The devices operated steadily regardless of the external conditions. Logger cases and observation wells maintained tightness, which points to the correct application of solutions protecting the electronic circuits against humidity.

Temperature indications for both study sites, although differing in particular temperature values (depending on the local meteorological and lithological conditions), showed similar trends of change in time and vertical profile. The highest temperature variability was observed for the shallowest sensors (0.05, 0.10 and 0.20 m). It remained in strict connection with the daily oscillations of air temperature. In the coolest periods, the soil temperature at the depth of 0.05 m was -3°C, whereas in the summer season it reached 29°C. Sensor indications pointed to the influence of the

snow cover’s insulating properties. During snow cover occurrence, the temperature noted by shallow sensors did not reveal oscillations related with daily fluctuations of the air temperature and remained at a level from about -1 to slightly above 0°C . Similar results were described in the paper of Dafflon et al. [38].

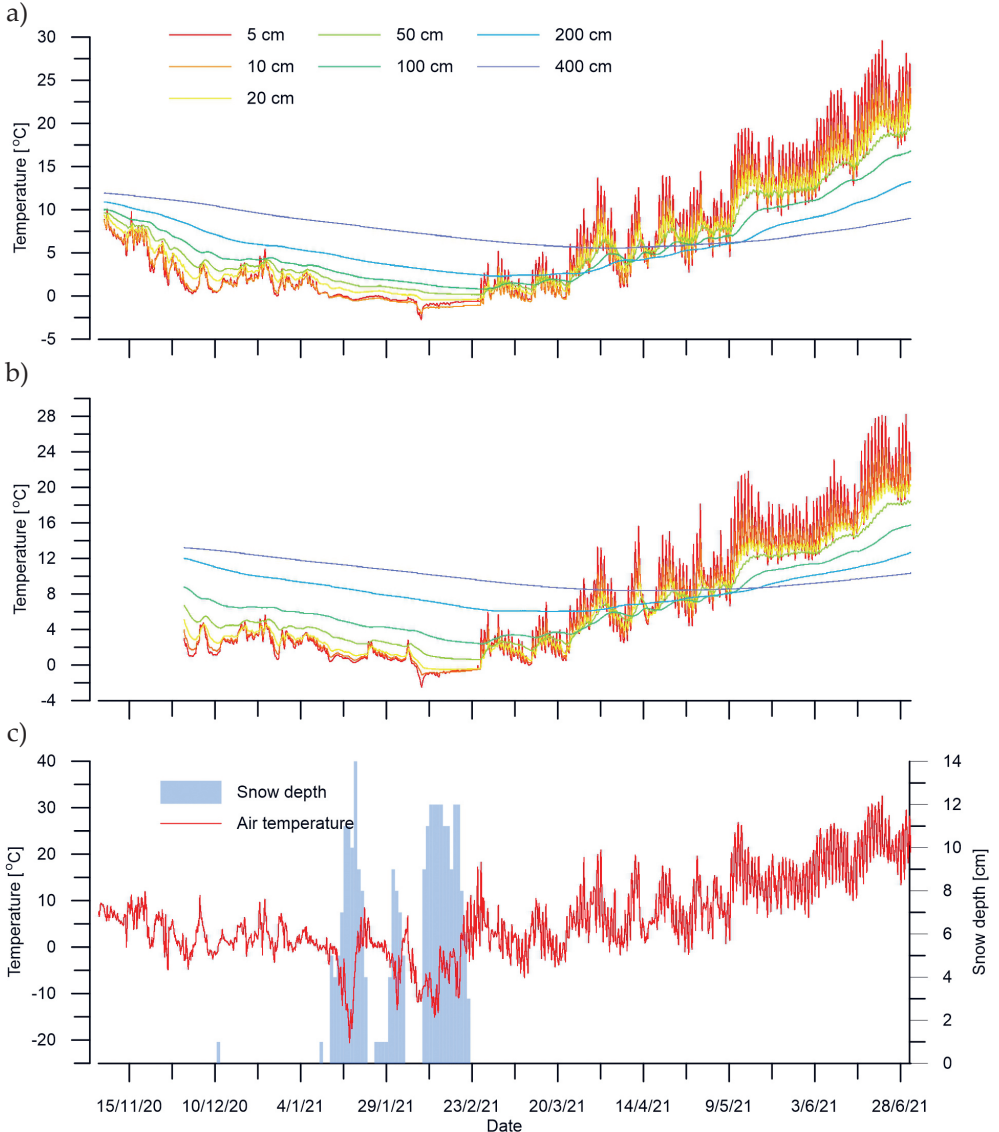


Fig. 8. Results of soil temperature measurements with a 10 min interval at depth levels of 0.05, 0.1, 0.2, 0.5, 1.0, 2.0 and 4.0 m in Bobrowce (a) and Warsaw (b) test points with regard to the daily mean air temperature and snow cover thickness in the IMGW Warszawa-Okęcie meteorological station (c)

With depth, the daily temperature fluctuations weakened and the registered temperature variability recalled long-term and seasonal fluctuations with a decreasing amplitude. For example, the differences between the highest and lowest temperature indications in the study interval at the depth of 2.0 m were 12.7°C (Bobrowce) and 8.2°C (Warsaw), whereas at the depth of 4.0 m the indications were 6.3 and 4.8°C, respectively. Phase shift between different depths could also be observed, which points to a delay in the propagation of the heat wave. This is particularly discernible in the indications of the sensors installed on 2.0 and 4.0 m below the surface, where the minimal temperature for the shallower sensor was registered about 1 month earlier than for the deepest sensor. These indications are in accordance with the theoretical model of heat wave propagation in the zone of seasonal fluctuations.

The next logger operation test included estimating the concordance of the temperatures registered at different depths of the soil medium with the theoretical model of heat wave propagation due to heat conduction. This allowed for the comparison of the measurement circuit in field conditions. In this case, the model described in chapter 2.4 was applied and which required the acceptance of several simplifying assumptions. It was presumed that the analyzed soil medium is homogenous and its thermal diffusivity is constant in time and space. Additionally, it was assumed that the horizontal temperature gradients are insignificantly small, due to which the process of heat conduction may be described with the application of a univariate model. Additionally, it was accepted that heat transfer caused by convection in the vadose zone may be omitted.

After solving a set of linear equations, a two-dimensional array of numbers was obtained representing the spatio-temporal distribution of temperature in the soil medium. The model was calibrated by subsequent approximations by picking values of heat diffusivity of the medium in order to minimize the differences between calculated and measured temperatures. Quantitative assessment of the match was made based on the calculated value of the mean absolute error (MAE in practice, this means that each of the models could be calibrated based on a dataset of 25,470 temperature measurements (hourly means) collected from depth levels 0.1, 0.2, 0.5, 1.0 and 2.0 m. The data could be compared with results of calculations collected from nodes corresponding to these depth levels (Figs. 9, 10). In both profiles studied, the theoretical temperature curve was very close to the curve obtained from the logger on each of the analyzed depth levels. This translates into the low value of the mean absolute error, which in the case of each sensor did not exceed 0.2°C (Tab. 2). It should be emphasized that these values, after calibration, are significantly below the measurement accuracy declared by the sensor producer. The obtained error values are satisfactorily low, particularly with regard to the simplifications accepted in the numerical model. Furthermore, drift was not observed in any sensor and differences between measured and calculated temperatures were on a similarly low level throughout the 7-month observation period.

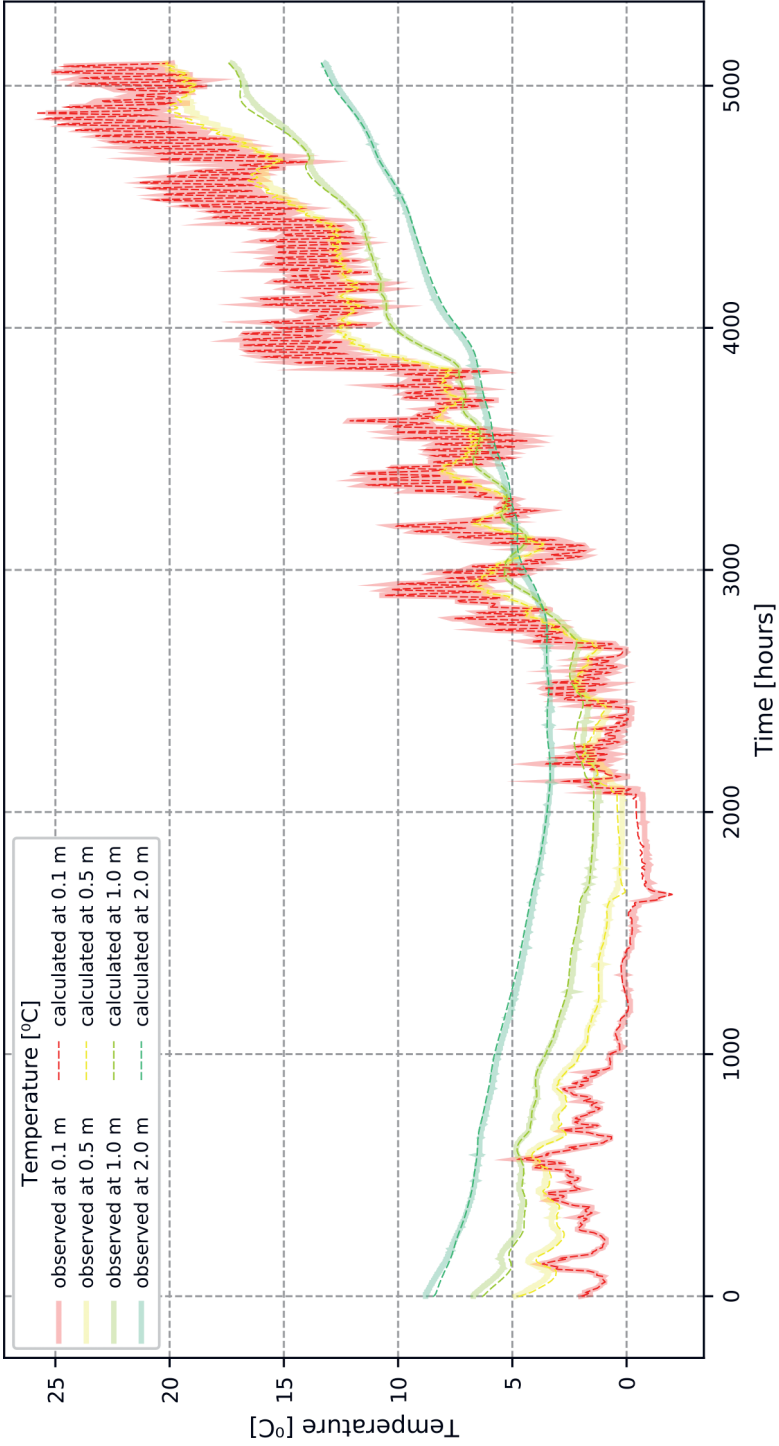


Fig. 9. Calculated and observed temperature of soil at different depths in the Bobrowce study site

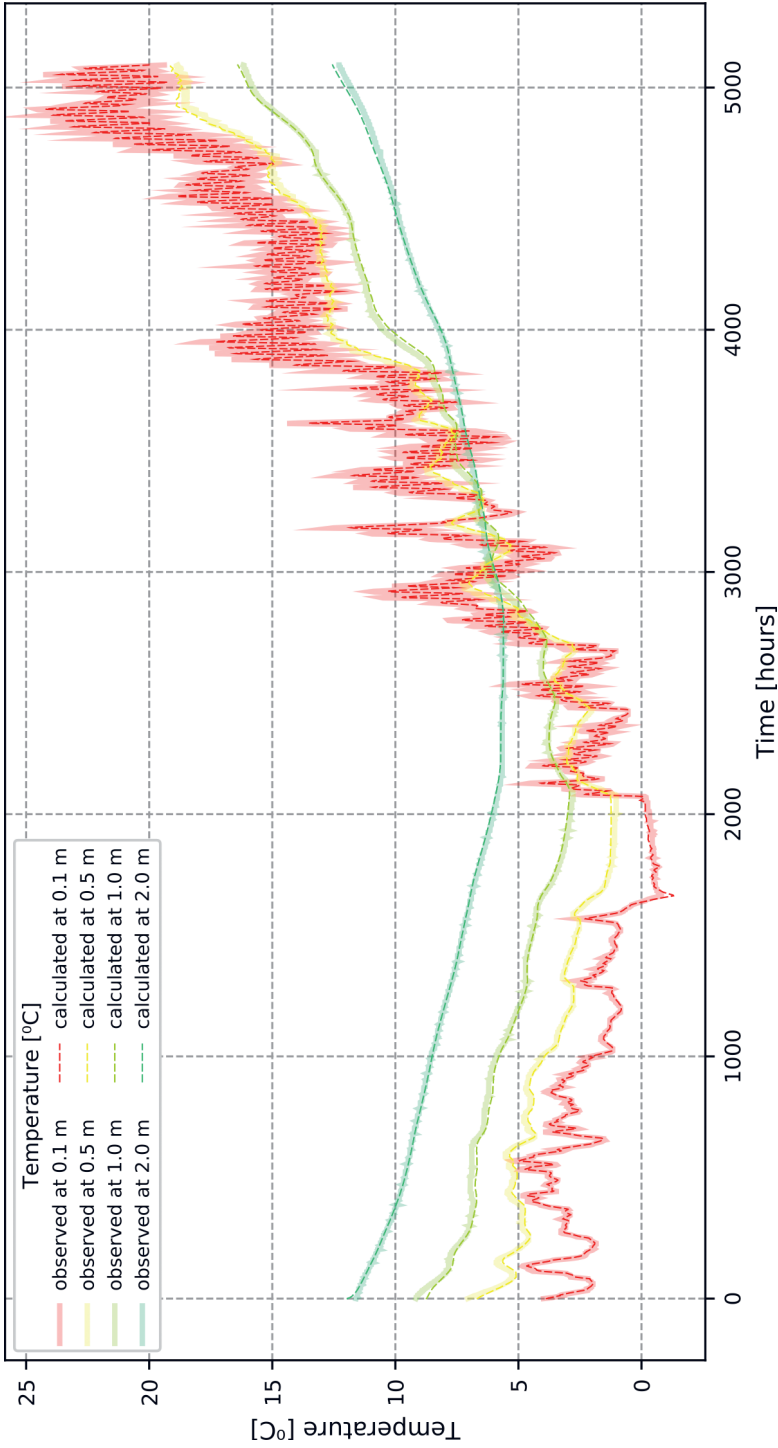


Fig. 10. Calculated and observed temperatures of soil at different depths in the Warsaw study site

Table 2. Values of mean absolute error [°C] determined on the basis of temperature recorded for individual sensors

Sensor depth [m]	Profile Bobrowce ($n_{\text{sensor}} = 5,095$) ($n_{\text{total}} = 25,470$)	Profile Warsaw ($n_{\text{sensor}} = 5,095$) ($n_{\text{total}} = 25,470$)
0.1	0.148	0.198
0.2	0.191	0.146
0.5	0.138	0.112
1.0	0.130	0.124
2.0	0.122	0.065
Total	0.146	0.129

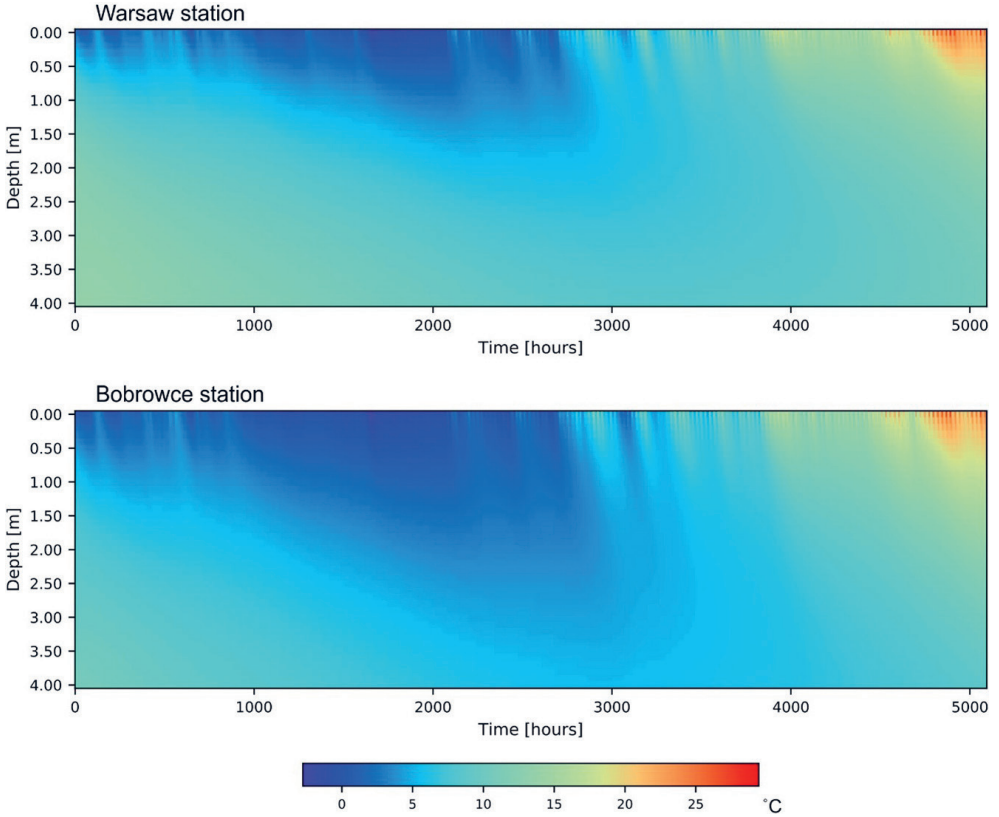


Fig. 11. Calculated temperature of the soil vs. time and depth at different values of thermal diffusivity ($1.28 \text{ m}^2/\text{d}$ in the Warsaw profile and $2.2 \text{ m}^2/\text{d}$ in the Bobrowce profile)

Following model calibration, the best fit in the Warsaw study site was obtained for heat diffusivity at the level of $0.0591 \text{ m}^2/\text{d}$, and in the Bobrowce site – at $0.1016 \text{ m}^2/\text{d}$. This diffusivity values are within the typical range reported for sandy clays and sands [39–43]. This variability is caused by the different lithology of the sediments in both sites, which has an impact on their different heat conductivity, specific heat and density. Variable heat diffusivity of the soil influences both the speed of heat wave propagation and its permittivity. Results of the model calculations (Fig. 11) indicate that in the analyzed depth zone, the variability of the soil temperature results from both the daily amplitude of surface temperature (high frequency signal), as well as seasonal variability observed on an annual basis (low frequency signal). The low heat diffusivity of the sediments in the Warsaw profile means that the speed of heat wave propagation is much lower than in the Bobrowce profile, for both low and high frequency signals. Additionally, the signal amplitude is attenuated here much faster, which influences low wave permittivity particularly in the case of high frequency signals.

3.4. Cost of the Measurement Kit

One of the assumptions during the development of the measurement-logging device was maintaining low production costs for both the logger and temperature sensors. The cost calculation presented in Table 3 for a single measurement-registration device presents individual prices of electric components indispensable for the project.

Table 3. List of manufacturing costs for a single set of data logger and temperature sensors in euro. Conversion from values expressed in Polish zloty (PLN) according to the exchange rate of 30.04.2021, provided by the National Bank of Poland.
The given prices include 22% VAT

Component name	Cost per unit [EUR]
Data logger unit	
Arduino Pro Mini (1 psc)	11.40
Micro SD module (1 psc)	1.78
Micro SD card (1 psc)	4.65
RTC DS3231 module (1 psc)	1.76
PCB with shipping to Poland	3.52
4 × AA battery holder (1 psc)	0.67
4 × AA lithium batteries	5.00
Hermetic case (1 psc)	4.62
6-pins hermetic connector (1 psc)	4.16
Connectors, resistors, capacitor, LED RGB, switches, wires, cable gromet	4.71
Sum: 42.27 EUR	

Table 3. cont.

Component name	Cost per unit [EUR]
Set of sensors	
DS18B20 sensors (7 pcs)	12.88
Covers for temperature sensor (7 pcs)	1.61
Cable grommets (7 pcs)	3.22
OZ600/3X0.5 wire (7 m)	6.58
Thermal silicone paste (10 g)	2.53
Epoxy 049 – two components (100 g)	4.63
Sum: 31.45 EUR	
Data logger observing well	
Pails round 5 liters (1 psc)	1.50
Cable grommet (1 psc)	0.46
Sum: 1.96 EUR	
Communication interface	
Serial Basic – converter USB-UART CH340G – SparkFun	8.81
MicroUSB B – A cabbles (1 psc)	8.84
6-pins hermetic connector (1 psc)	3.63
Sum: 21.28 EUR	
Total sum: 96.96 EUR	

The total cost also includes an additional circuit for communication between the logger and PC. This is a single cost as the circuit may be used for the entire measurement network. After subtracting costs related with the communication interface, the value of a single kit is about 76 EUR (calculated on 30.04.2021). This is a competitive value in comparison with commercial solutions.

4. Conclusions

The paper presents the design, construction, and tests of a device for long-term soil temperature measurement and logging. The presented data logger is based on an AVR microcontroller mounted on an Arduino Pro Mini circuit board. The temperature sensors used in the project are digital DS18B20 thermometers.

Prototype measurement devices were tested in laboratory and field conditions. The assessment of their operation was conducted in two ways: to test the efficiency

of the circuit and to test the correctness of data measured by seven sensors installed at different depth levels. To achieve this, the measurement-registration devices were installed in two study sites in deposits differing in lithology. The tests were conducted during a 7-month interval. Prior to installation, all sensors were subject to calibration in laboratory conditions. The calibration allowed to reach an accuracy of about $\pm 0.1^{\circ}\text{C}$. This value is in accordance with the standards of temperature sensor accuracy determined by WMO.

Tests of the logging system gave positive results. The device is autonomous, durable, and stable, and its estimated operation time on one battery set is about 300 days in temperate weather conditions. The device operated without flaws both at sub-zero temperatures reaching down to -20°C , as well as high temperatures of up to 30°C . No errors were observed in the system of data reading from DS18B20 sensors, as well as their saving and cyclic record for archiving and control. The applied case is tight and successfully protects the electronic components against humidity. The logger is universal in nature and after appropriate changes in the executed code may be used for data logging from other sensors than those implemented for soil temperature surveys. It should be emphasized, however, that the microcontroller restricted resources with regard to timing, available memory for the programme, and operation memory.

Model surveys have shown that temperature indications from the sensors are in accordance with the theoretical spatio-temporal distribution of soil temperature shaped by conduction. In practice, this means that the datasets obtained from the developed measurement device may be used for tasks realized with the application of a mathematical model. This expands the perspectives of using the measurement system in shallow geothermal technologies, and the data acquired by the device may be used for both heat pumps optimization and the identification of soil heat diffusivity. Additionally, the sensors may be used in other spatial configurations than those presented in this report. This creates potential possibilities of using measurement sets for the analysis of heat flow processes due to conduction and convection in 2D and 3D space, and the possible heterogeneity of the medium.

The calculated cost of the sensor set and the logging device is 76 EUR. This amount is competitive with regard to the available commercial solutions. It allows for the construction, mounting, and service of the monitoring system. Due to this fact, the measurement systems may be developed at relatively low costs and the acquired datasets will facilitate user analysis of the heat flow processes at high temporal and spatial resolutions.

Author Contributions

Author 1: design and construction of the measuring and recording system, device programming, data analysis, manuscript writing.

Author 2: developing an algorithm for data interpretation, data analysis, manuscript writing.

References

- [1] Teleszewski T.J., Krawczyk D.A., Fernandez-Rodriguez J.M., Lozano-Lunar A., Rodero A.: *The study of soil temperature distribution for very low-temperature geothermal energy applications in selected locations of temperate and subtropical climate*. *Energies*, vol. 15(9), 2022, 3345. <https://doi.org/10.3390/en15093345>.
- [2] Horton R., Wierenga P.J., Nielsen D.R.: *Evaluation of methods for determining the apparent thermal diffusivity of soil near the surface*. *Soil Science Society of America Journal*, vol. 47(1), 1983, pp. 25–32. <https://doi.org/10.2136/sssaj1983.03615995004700010005x>.
- [3] An K., Wang W., Zhao Y., Huang W., Chen L., Zhang Z., Wang Q., Li W.: *Estimation from soil temperature of soil thermal diffusivity and heat flux in sub-surface layers*. *Boundary-Layer Meteorology*, vol. 158, 2016, pp. 473–488. <https://doi.org/10.1007/s10546-015-0096-7>.
- [4] Yang L., Song R., Dong B., Yin L., Fan Y., Zhang B., Wang Z., Wang Y., Dong S.: *Processing method of soil temperature time series and its application in geothermal heat flow*. *Frontiers in Earth Science*, vol. 10, 2022, 910328. <https://doi.org/10.3389/feart.2022.910328>.
- [5] Seward A., Prieto A.: *Determining thermal rock properties of soils in Canterbury, New Zealand: Comparisons between long-term in-situ temperature profiles and divided bar measurements*. *Renewable Energy*, vol. 118, 2018, pp. 546–554. <https://doi.org/10.1016/j.renene.2017.11.050>.
- [6] Gruszczyński T., Szostakiewicz-Hołownia M.: *Interpretacja zmienności temperatury wody w źródle na wschodnim stoku Zameczków (Tatry Zachodnie) na podstawie ciągłych obserwacji monitoringowych i numerycznego modelu transportu ciepła*. *Biuletyn Państwowego Instytutu Geologicznego*, vol. 475, 2019, pp. 43–50. <https://doi.org/10.7306/bpig.5>.
- [7] ONSET: *Outdoor Monitoring Solutions. Onset HOBO data loggers set the standard for reliable, accurate data logging for outdoor monitoring applications*. <https://www.onsetcomp.com/outdoor-monitoring-solutions/> [access: 24.08.2022].
- [8] Davis Instruments. <https://www.davisinstruments.com/pages/data-collection> [access: 24.08.2022].
- [9] Maxim Integrated: *iButton High-Capacity Temperature Logger with 122KB Data-Log Memory*. <https://datasheets.maximintegrated.com/en/ds/DS1925.pdf> [access: 24.08.2022].
- [10] Vickers M., Schwarzkopf L.: *A simple method to predict body temperature of small reptiles from environmental temperature*. *Ecology and Evolution*, vol. 6(10), 2016, pp. 3059–3066. <https://doi.org/10.1002/ece3.1961>.
- [11] Gandra M., Seabra R., Lima F.P.: *A low-cost, versatile data logging system for ecological applications*. *Limnology and Oceanography: Methods*, vol. 13(3), 2015, pp. 115–126. <https://doi.org/10.1002/lom3.10012>.

-
- [12] Ferlan M., Simončič P.: *Robust and cost-effective system for measuring and logging of data on soil water content and soil temperature profile*. *Agricultural Sciences*, vol. 3(6), 2012, pp. 865–870. <https://doi.org/10.4236/as.2012.36105>.
- [13] Lockridge G., Dzwonkowski B., Nelson R., Powers S.: *Development of a low-cost arduino-based sonde for coastal applications*. *Sensors (Switzerland)*, vol. 16(4), 2016, 528. <https://doi.org/10.3390/s16040528>.
- [14] Akhter T., Ali M., Cha J., Park S., Jang G., Yang K., Kim H.: *Development of a data acquisition system for the long-term monitoring of plum (Japanese apricot) farm environment and soil*. *Journal of Biosystems Engineering*, vol. 43(4), 2018, pp. 426–439.
- [15] Fisher D.K., Woodruff L.K., Anapalli S.S., Pinnamaneni S.R.: *Open-source wireless cloud-connected agricultural sensor network*. *Journal of Sensor and Actuator Networks*, vol. 7(4), 2018, 47. <https://doi.org/10.3390/jsan7040047>.
- [16] Medojevic M., Medojevic M., Radakovic N., Lazarevic M., Sremcevic N.: *A conceptual solution of low-cost temperature data logger with relatively high accuracy*. *International Journal of Industrial Engineering and Management*, vol. 9(1), 2018, pp. 53–58.
- [17] Beddows P.A., Mallon E.K.: *Cave pearl data logger: A flexible arduino-based logging platform for long-term monitoring in harsh environments*. *Sensors (Switzerland)*, vol. 18(2), 2018, 530. <https://doi.org/10.3390/s18020530>.
- [18] Mallon E.K.: *The Cave Pearl Project*. <https://thecavepearlproject.org/> [access: 7.02.2022].
- [19] World Meteorological Organization: *Guide to Instruments and Methods of Observation (WMO-No. 8) Volume I: Measurement of Meteorological Variables*. WMO, 2018.
- [20] Arduino. <https://www.arduino.cc/> [access: 24.08.2022].
- [21] Atmel: *ATmega328P: 8-bit AVR Microcontroller with 32K Bytes In-System Programmable Flash. Datasheet*. http://ww1.microchip.com/downloads/en/Device-Doc/Atmel-7810-Automotive-Microcontrollers-ATmega328P_Datasheet.pdf [access: 9.02.2021].
- [22] Damanik N., Robiansyah M.R., Apriliana A., Purba S.: *Design of energy monitoring system for small scale wind turbine applications*. *IOP Conference Series: Earth and Environmental Science*, vol. 345, 2019, 012003. <https://doi.org/10.1088/1755-1315/345/1/012003>.
- [23] Maxim Integrated: *Extremely Accurate I2C-Integrated RTC / TCXO / Crystal*. <https://datasheets.maximintegrated.com/en/ds/DS3231.pdf> [access: 9.02.2021].
- [24] Ali A.S., Zanzinger Z., Debose D., Stephens B.: *Open Source Building Science Sensors (OSBSS): A low-cost Arduino-based platform for long-term indoor environmental data collection*. *Building and Environment*, vol. 100, 2016, pp. 114–126. <https://doi.org/10.1016/j.buildenv.2016.02.010>.

- [25] Borecka A., Sekuła K., Kessler D., Majerski P.: *Zastosowanie testowych czujników pomiaru temperatury w quasi-przestrzennych (3D) sieciach pomiarowych w hydrotechnicznych budowlach ziemnych – wyniki wstępne* [Application of testing temperature sensors for quasi-dimensional (3D) measurement systems used in measuring hydrotechnical earthworks – preliminary results]. *Przeegląd Geologiczny*, vol. 65(10/2), 2017, pp. 748–755.
- [26] Cifuentes H., Montero-Chacón F., Galán J., Cabezas J., Martínez-De la Concha A.: *A finite element-based methodology for the thermo-mechanical analysis of early age behavior in concrete structures*. *International Journal of Concrete Structures and Materials*, vol. 13, 2019, 41. <https://doi.org/10.1186/s40069-019-0353-0>.
- [27] Zhao X., Li W., Zhou L., Song G.-B., Ba Q., Ou J.: *Active thermometry based DS18B20 temperature sensor network for offshore pipeline scour monitoring using K-means clustering algorithm*. *International Journal of Distributed Sensor Networks*, vol. 9(6), 2013, pp. 1–11. <https://doi.org/10.1155/2013/852090>.
- [28] Blázquez C.S., Piedelobo L., Fernández-Hernández J., Nieto I.M., Martín A.F., Lagüela S., González-Aguilera D.: *Novel experimental device to monitor the ground thermal exchange in a borehole heat exchanger*. *Energies*, vol. 13(5), 2020, 1270. <https://doi.org/10.3390/en13051270>.
- [29] Le A.T., Wang L., Wang Y., Li D.: *Measurement investigation on the feasibility of shallow geothermal energy for heating and cooling applied in agricultural greenhouses of Shouguang City: Ground temperature profiles and geothermal potential*. *Information Processing in Agriculture*, vol. 8(2), 2021, pp. 251–269. <https://doi.org/10.1016/j.inpa.2020.06.001>.
- [30] Chen M.K., Li W.B., Kan J.M.: *Remote multi-layer soil temperature monitoring system based on GPRS*. *Sensors and Transducers*, vol. 164(2), 2014, pp. 107–113.
- [31] Gao W., Wang X., Zeng M., Han C.: *Observation scheme for temperature and deformation of permafrost subgrade in Yichun-Bei'an Highway*. *IOP Conference Series: Earth and Environmental Science*, vol. 267, 2019, 052003. <https://doi.org/10.1088/1755-1315/267/5/052003>.
- [32] Larwa B.: *Investigation of temperature distribution in the ground induced by heat source and under natural conditions*. *Technical Transactions*, vol. 10, 2017, pp. 69–77. <https://doi.org/10.4467/2353737xct.17.177.7285>.
- [33] Maxim Integrated: *DS18B20 Programmable Resolution 1-Wire Digital Thermometer*. <https://datasheets.maximintegrated.com/en/ds/DS18B20.pdf> [access: 9.02.2021].
- [34] Maxim Integrated: *Curve Fitting the Error of a Bandgap-Based Digital Temperature Sensor*. <https://www.maximintegrated.com/en/design/technical-documents/app-notes/2/208.html> [access: 12.05.2021].
- [35] Zaszewski D.: *Low-cost automatic system for long-term observations of soil temperature – supplementary materials*. *Mendeley Data*, V1, 2022. <https://doi.org/10.17632/k5w4v6h5cp.1>.

-
- [36] Energizer: *Cylindrical Primary Lithium Handbook and Application Manual*. https://data.energizer.com/pdfs/lithiuml91192_appman.pdf [access: 31.03.2021].
- [37] Burton M.: *Arduino Temperature Control Library*. <https://github.com/milesburton/Arduino-Temperature-Control-Library> [access: 24.08.2022].
- [38] Dafflon B., Wielandt S., Lamb J., McClure P., Shirley I., Uhlemann S., Wang C. et al.: *A distributed temperature profiling system for vertically and laterally dense acquisition of soil and snow temperature*. *The Cryosphere*, vol. 16, 2022, pp. 719–736. <https://doi.org/10.5194/tc-16-719-2022>.
- [39] Abu-Hamdeh N.H.: *Thermal properties of soils as affected by density and water content*. *Biosystems Engineering*, vol. 86(1), 2003, pp. 97–102. [https://doi.org/10.1016/S1537-5110\(03\)00112-0](https://doi.org/10.1016/S1537-5110(03)00112-0).
- [40] Arkhangelskaya T.A.: *Parameters of the thermal diffusivity vs. water content function for mineral soils of different textural classes*. *Eurasian Soil Science*, vol. 53, 2020, pp. 39–49. <https://doi.org/10.1134/S1064229320010032>.
- [41] Márquez J.M.A., Bohórquez M.Á.M., Melgar S.G.: *Ground thermal diffusivity calculation by direct soil temperature measurement. application to very low enthalpy geothermal energy systems*. *Sensors (Switzerland)*, vol. 16(3), 2016, 306. <https://doi.org/10.3390/s16030306>.
- [42] Busby J.: *Thermal conductivity and diffusivity estimations for shallow geothermal systems*. *Quarterly Journal of Engineering Geology and Hydrogeology*, vol. 49(2), 2016, pp. 138–146. <https://doi.org/10.1144/qjegh2015-079>.
- [43] Thomson J.: *Observations of thermal diffusivity and a relation to the porosity of tidal flat sediments*. *Journal of Geophysical Research: Oceans*, vol. 115(C5), 2010, C05016. <https://doi.org/10.1029/2009JC005968>.